Capture of carbon dioxide from flue or fuel gas mixtures by clathrate crystallization in a silica gel column

Adeyemo, Adebola; Kumar, Rajnish; Linga, Praveen; Ripmeester, John; Englezos, Peter

Publisher's version / Version de l'éditeur:
https://doi.org/10.1016/j.ijggc.2009.11.011
International journal of greenhouse gas control, 4, May 3, pp. 478-485, 2010-05-01

International Journal of Greenhouse Gas Control xxx (2009) xxx–xxx

Contents lists available at ScienceDirect

International Journal of Greenhouse Gas Control

journal homepage: www.elsevier.com/locate/ijggc

Capture of carbon dioxide from flue or fuel gas mixtures by clathrate crystallization in a silica gel column

Adebola Adeyemo [a,b], Rajnish Kumar [a,b], Praveen Linga [a], John Ripmeester [b], Peter Englezos [a,*]

[a] Department of Chemical and Biological Engineering, University of British Columbia, 2360 East Mall, Vancouver, BC, Canada V6T 1Z3
[b] Steacie Institute for Molecular Sciences, National Research Council Canada, Ottawa, ON, Canada K1A 0R6

ARTICLE INFO

Article history:
Received 22 July 2009
Received in revised form 1 October 2009
Accepted 22 November 2009

Keywords:
Gas hydrate
Silica gel
Carbon dioxide capture
Flue gas
Hydrogen
Gas separation

ABSTRACT

A column of silica gel was employed to contact water with flue gas (CO_2/N_2) mixture to assess if CO_2 can be separated by hydrate crystallization. Three different silica gels were used. One with a pore size of 30 nm (particle size 40–75 μm) and two with a pore size of 100 nm and particle sizes of 40–75 and 75–200 μm respectively. The observed trends indicate that larger pores and particle size increase the gas consumption, CO_2 recovery, separation factor and water conversion to hydrate. Thus, the gel (gel #3) with the larger particle size and larger pore size was chosen to carry out experiments with concentrated CO_2 mixtures and for experiments in the presence of tetrahydrofuran (THF), which itself is a hydrate forming substance. Addition of THF reduces the operating pressure in the crystallizer but it also reduces the gas uptake. Gel #3 was also used in experiments with a fuel gas (CO_2/H_2) mixture in order to recover CO_2 and H_2. It was found that the gel column performs as well as a stirred reactor in separating the gas components from both flue gas and fuel gas mixtures. However, the crystallization rate and hydrate yield are considerably enhanced in the former. Finally the need for stirring is eliminated with the gel column which is enormously beneficial economically.

1. Introduction

Capture of CO_2 from power plant flue gases from conventional power plants or from fuel gases from gasification plants is a technological application of gas hydrates under consideration (Aaron and Tsouris, 2005; Kang and Lee, 2000; Klara and Srivastava, 2002; Kumar et al., 2009; Linga et al., 2008, 2007a; Seo et al., 2005). Post-combustion CO_2 capture involves separation of CO_2 from the flue gas mixture emitted from a power plant. A typical pretreated flue gas contains 15–20 mol% CO_2, 5–9% O_2, and the rest N_2. A process combining three hydrate crystallization stages and a membrane separation stage has been proposed for the capture of carbon dioxide from such mixtures (Linga et al., 2008, 2007a). On the other hand pre-combustion capture involves separation of carbon dioxide from a carbon dioxide/hydrogen mixture (Herzog and Drake, 1996; Klara and Srivastava, 2002). A typical fuel gas mixture is a mixture of predominantly H_2 (~60 mol%) and CO_2 (~40 mol%) (Booras and Smelser, 1991; Hendriks et al., 1991) coming out from an integrated gasification combined cycle (IGCC) at a pressure of 2.5–7 MPa (IPCC, 2005). This fuel gas mixture is pretreated for removal of particulate matter and H_2S.

The above proposed processes were based on laboratory-scale data employing stirred vessels as crystallizers. Agglomeration of hydrate crystals creates barriers to efficient gas/water contacting in such crystallizers and as a result the rate of crystallization decreases and the conversion of water and gas to hydrate is limited (Englezos, 1996; Lee et al., 2005; Linga et al., 2007b). For example, a 4% conversion at the onset of agglomeration has been reported (Englezos, 1996). There is an ongoing effort to improve the performance of these crystallizers that will enable the continuous and efficient hydrate crystallization for CO_2 capture, natural gas storage and transport and other gas separation applications like separation of HFC-134a (Nagata et al., 2009). Mori (2003) reviewed and discussed the various hydrate formation vessels and their limitations. For example, other arrangements such as bubbles dispersed in water or water droplets injected into a gas atmosphere have been proposed (Gudmundsson et al., 2000; McCallum et al., 2007; Ohmura et al., 2002; Tsuji et al., 2004). Tsouris and co-workers have presented novel and efficient crystallizers in the context of CO_2 sequestration work (Lee et al., 2003; Tsouris et al., 2004, 2007; West et al., 2001). In addition, it has also been reported that when hydrate is formed from ice, temperature ramping enhances the conversion (Susilo et al., 2007b; Wang et al., 2002).

Another method to overcome the gas/water contact limitation is to contact the gas phase with water dispersed in the pores of silica gel and have the hydrate formed within the pores (Adeyemo,

* Corresponding author. Tel.: +1 604 822 6184; fax: +1 604 822 6003.
E-mail address: englezos@interchange.ubc.ca (P. Englezos).

1750-5836/$ – see front matter © 2009 Elsevier Ltd. All rights reserved.
doi:10.1016/j.ijggc.2009.11.011

2008; Kang et al., 2008; Park et al., 2006; Seo et al., 2005). Porous materials such as silica gel possess high internal surface area per volume. An additional benefit of using porous materials compared to stirred vessels is that there is no need for power consumption due to stirring. Thus, the objective of the present study is to investigate the effectiveness of the silica gel bed for the separation of CO_2 from CO_2/N_2 (flue gas) and CO_2/H_2 (fuel gas) mixtures through hydrate crystallization.

2. Experimental

2.1. Materials

The gas mixtures were ultra high purity (UHP) grade and supplied by Praxair Technology Inc. The dry molar (%) gas compositions of the binary gas mixtures were determined by gas chromatography and are as follows: CO_2 (17.0)/N_2 (83.0) for the model flue gas and CO_2 (40.0)/H_2 (60%) for the model fuel gas mixture. Since N_2 and O_2 form hydrate at approximately the same pressure/temperature conditions, the above CO_2/N_2 mixture is considered a suitable model flue gas (Kang and Lee, 2000; Linga et al., 2007a). THF was supplied by Fisher Scientific with 99% purity. Distilled and deionized water was used. Three gels from Silicycle (Canada) were used. Table 1 summarizes the properties of all the three gels used in this work. A Micromeritics ASAP 2010 pore size analyzer was used to confirm the properties of the gels. Pore volume was determined based on BET analysis.

2.2. Apparatus

The apparatus is shown in Fig. 1. The hydrate crystallizer or reactor (HR) is made of stainless steel (316) with an internal volume of 227 cm^3. HR has a coiled copper tubing inside through which cooling fluid is circulated to remove heat evolving from hydrate formation. Four T-type thermocouples (Omega) are used to monitor temperature in the gel matrix. A pressure gauge (Dwyer digital, DPG-100) is connected to the reactor. Hydrate formation experiments are conducted in a semi-batch manner at constant pressure and temperature. The gas from vessel (SV) is supplied continuously at constant pressure to the reactor containing a fixed amount of water. The supply vessel and the reactor are located inside the temperature controlled water bath (WB). A BROOKS 5860S/BC (accuracy ±0.7% of flow rate) mass flow meter (FM1) is used to measure the quantity of gas supplied to the reactor. A second flow meter (FM2) is used to measure the quantity of gas released from hydrate during decomposition.

2.3. Experimental procedure and operating conditions

The procedure for gel preparation was as follows. Each gel was first dried at 373 K for 24 h and then weighed to determine the dry weight silica. Water equal to the pore volume of the silica gel was then added to the dried silica to obtain pore saturated silica gel. Pore volume was determined based on BET analysis. Accordingly, 35 ml of water was added to saturate the gel pore with water. The gel was then placed in a Geneq centrifuge and spun at 3000 rpm for 3 min to aid the dispersion of water. From visual observation and thermo-gravimetric analysis of various samples, it was found that water was evenly dispersed in the silica gel (Adeyemo, 2008).

The reactor was now charged with ~100 cm^3 of silica gel saturated with water. Prior to commencing the kinetic experiment, two cycles of hydrate formation and decomposition were carried out. This ensured that the water in the gel matrix exhibited the 'memory' effect that is generally accepted to shorten induction times (Lee et al., 2005; Uchida et al., 2000). The reactor was then pressurized to the desired pressure. As hydrate formation proceeds causing a pressure drop in the reactor, gas flows from the supply vessel to maintain the constant pressure in the reactor. Each experiment was run for 4 h after which final gas and hydrate phase compositions were determined. Gas samples (300 μL) were taken every 30 min for analysis with the Gas Chromatography (GC).

Table 1
Silica gel properties.

Silica gel type	Particle size distribution (μm)	Pore diameter (nm)	Pore volume (ml/g)	Surface area (m^2/g)
#1	45–75	30.0	0.81	100
#2	45–75	100.0	0.81	50
#3	75–200	100.0	0.83	50

For a 17% CO_2/N_2 mixture, equilibrium formation pressure of ~6.0 MPa at 271.3 K was reported for 30 nm silica gel pore size by Seo et al. (2005). Based on these results, experiments were designed to run at 272.15 K, with operating pressures of 8.0 and 9.0 MPa respectively. Analysis with a differential scanning calorimeter indicated that the water confined in silica gel pores exhibited freezing point depression and thus remained in the liquid state at 272.15 K (Adeyemo, 2008). The experiments with THF and the 17% CO_2 flue gas were carried out at 5 MPa and 272.1 K. The experiments with the CO_2/H_2 mixture and the CO_2/H_2/THF (1 mol%) system were conducted at 7.0 and 5.0 MPa respectively.

At the end of hydrate formation (240 min), hydrate was dissociated by isolating the reactor from the supply vessel, and then depressurizing to atmospheric pressure and allowing the gas evolved from the hydrate to be collected in the reservoir (DG). GC was then used to determine the composition of the evolved gas.

2.4. Conversion of water to hydrate

Conversion of water to hydrate is determined by using the following equation:

$$\text{Conversion of water to hydrates (mol\%)} = \frac{\Delta n_{H,\downarrow} \times \text{hydration number}}{n_{H_2O}} \times 100 \quad (1)$$

where $\Delta n_{H,\downarrow}$ is the number of moles of gas consumed for hydrate formation at the end of the experiment determined from the gas uptake and n_{H_2O} is the total number of moles of water in the system. The hydration number is the number of water molecules per guest molecule. It can be determined experimentally by simultaneously using powder X-ray diffraction and Raman spectroscopy on solid hydrate phase (Kumar et al., 2009; Kumar et al., 2008; Sum et al., 1997; Susilo et al., 2007a; Uchida et al., 1999; Udachin et al., 2007, 2001) or by solid state NMR spectroscopy (Davidson et al., 1983; Ripmeester and Ratcliffe, 1988).

In the presence of THF, the conversion of water to hydrate is determined by the next equation

$$\text{Conversion of water to hydrates (mol\%)} = \frac{(\Delta n_{H,\downarrow} + \Delta n_{THF}) \times \text{hydration number}}{n_{H_2O}} \times 100 \quad (2)$$

where, Δn_{THF} is the number of moles of THF consumed for hydrate formation at the end of the experiment. Δn_{THF} is calculated based on the occupancy ratio for sII and the hydration number as follows:

$$\Delta n_{THF} = \text{hydration number} \times \frac{(\text{number of large cages}/\text{number of small cages})}{\text{hydration number for full occupancy}} \quad (3)$$

The hydration numbers used in the above equations are given in Table 2.

Please cite this article in press as: Adeyemo A, et al. Capture of carbon dioxide from flue or fuel gas mixtures by clathrate crystallization in a silica gel column. Int. J. Greenhouse Gas Control (2009), doi:10.1016/j.ijggc.2009.11.011

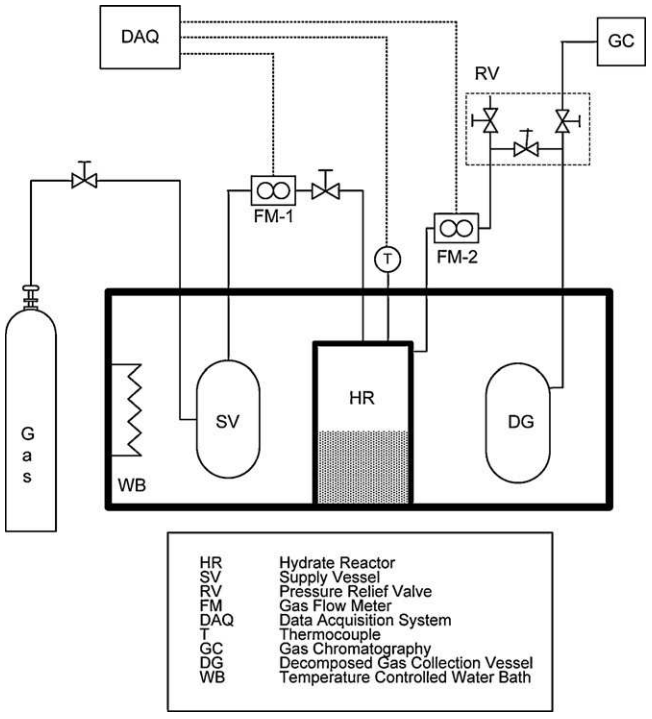

Fig. 1. Apparatus.

2.5. CO_2 recovery and efficiency

The CO_2 *recovery or split fraction* (S.Fr.) of CO_2 in gaseous and hydrate phase is calculated as follows (Linga et al., 2007a)

$$\text{S.Fr.} = \frac{n^{\text{H}}_{\text{CO}_2}}{n^{\text{Feed}}_{\text{CO}_2}} \tag{4}$$

where $n^{\text{Feed}}_{\text{CO}_2}$ is defined as number of moles of CO_2 in feed gas and $n^{\text{H}}_{\text{CO}_2}$ is the number of moles of CO_2 in hydrate phase at the end of the experiment. In addition, the separation factor (S.F.) is determined from the following equation (Linga et al., 2007a):

$$\text{S.F.} = \frac{n^{\text{H}}_{\text{CO}_2} \times n^{\text{gas}}_{\text{N}_2}}{n^{\text{H}}_{\text{N}_2} \times n^{\text{gas}}_{\text{CO}_2}} \tag{5}$$

where $n^{\text{gas}}_{\text{CO}_2}$ is the number of moles of CO_2 in the gas phase at the end of the kinetic experiment, $n^{\text{gas}}_{\text{N}_2}$ is the number of moles of N_2 in the gas phase at the end of the kinetic experiment and $n^{\text{H}}_{\text{N}_2}$ is the number of moles of N_2 in the hydrate phase.

3. Results and discussion

3.1. Post-combustion capture

3.1.1. Gas uptake and phase composition measurements

The progress of the hydrate crystallization process is monitored by determining the mass of gas consumed during a kinetic experiment. This is known as the gas uptake (Bishnoi and Natarajan, 1996). Fig. 2 shows the gas uptake at 8 and 9 MPa respectively and a 30 nm silica gel is used in the column (gel #1). As expected a higher gas consumption indicating increased hydrate formation is observed at 9 MPa compared to 8 MPa. It is also seen that, the gas consumption for the experiment conducted at 8.0 MPa for gel #1 slows down towards a plateau. Therefore, it was decided that the duration of the experiments be 240 min. The gas phase composition was analyzed during the kinetic experiment at different times, the CO_2 composition is given in Table 3. The CO_2 concentration in the gas phase was found to reduce from 17% to 14.9% and 14.70% for the 8 and 9 MPa experiments respectively conducted for the 30 nm silica gel (Table 3).

Fig. 3 shows the gas uptake results for the 100 nm gel (gel #2) at 8 and 9 MPa respectively. A similar trend of increased hydrate formation at 9 MPa compared to 8 MPa can be seen for gel #2. It is

Table 2
Summary of experiments conditions along with the calculated conversion of water to hydrates.

System	Exp. No.	Gel	P_{exp} (MPa)	T_{exp} (K)	End of experiment			
					Time (min)	Moles	Hydration number	Conversion of water to hydrate (%)
CO_2 (17.0%)/N_2 (83.0%)/water	1	#1	9.0	272.15	240.0	0.0453	6.28[a]	14.65
	2		9.0	272.15	240.0	0.0453		14.64
	3		8.0	272.15	240.0	0.0181		5.84
	4	#2	9.0	272.15	240.0	0.1261		40.72
	5		8.0	272.15	240.0	0.0932		30.09
	6	#3	9.0	272.15	240.0	0.1377		44.48
	7		9.0	272.15	240.0	0.1381		44.61
	8		8.0	272.15	240.0	0.0952		30.74
	9		8.0	272.15	240.0	0.0999		32.25
CO_2 (45.0%)/N_2 (55.0%)/water	10	#3	5.0	272.15	240.0	0.1336	6.24[b]	42.88
	11	#3	5.0	272.15	240.0	0.1376		44.17
CO_2 (71.0%)/N_2 (29.0%)/water	12	#3	2.7	272.15	240.0	0.1012	6.29[b]	32.70
	13	#3	2.7	272.15	240.0	0.0963		31.13
CO_2 (17.0%)/N_2 (83.0%)/1.0 mol% THF	14	#3	5.0	272.15	240.0	0.0196	5.71[a]	8.65
	15	#3	5.0	272.15	240.0	0.0198		8.73
	16	#3	5.0	274.15	240.0	0.0219		9.63
	17	#3	5.0	274.15	240.0	0.0223		9.84
CO_2 (40.0%)/H_2 (60.0%)/water	18	#3	7.0	272.15	240.0	0.0849	7.09[c]	30.94
	19	#3	7.0	272.15	240.0	0.0818		29.84
CO_2 (40.0%)/H_2 (60.0%)/1.0 mol% THF	20	#3	5.0	274.15	240.0	0.0175	10.05[d]	9.05

[a] From Kang et al. (2001).
[b] From CSMYD available in Sloan (1998).
[c] From Kumar et al. (2009).
[d] Same value as for $CO_2/H_2/C_3H_8$ given in Kumar et al. (2009) since THF occupies the large cages like propane in sII hydrate.

Please cite this article in press as: Adeyemo A, et al. Capture of carbon dioxide from flue or fuel gas mixtures by clathrate crystallization in a silica gel column. Int. J. Greenhouse Gas Control (2009), doi:10.1016/j.ijggc.2009.11.011

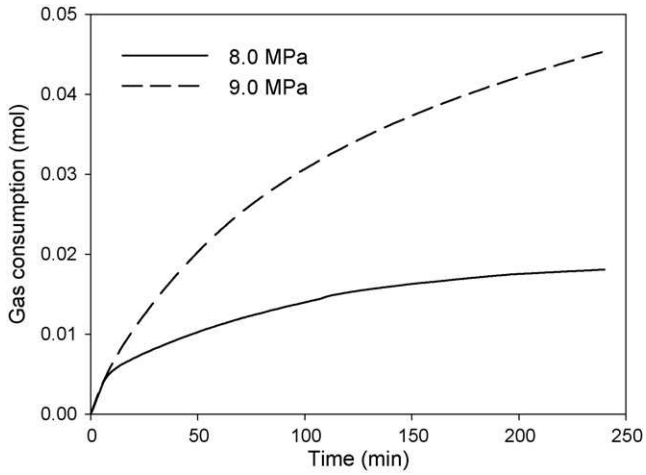

Fig. 2. Gas uptake measurement curves for hydrate formation in 30.0 nm silica gel pores (gel #1) at 272.15 K and 8.0 MPa (experiment 3) and 9.0 MPa (experiment 1).

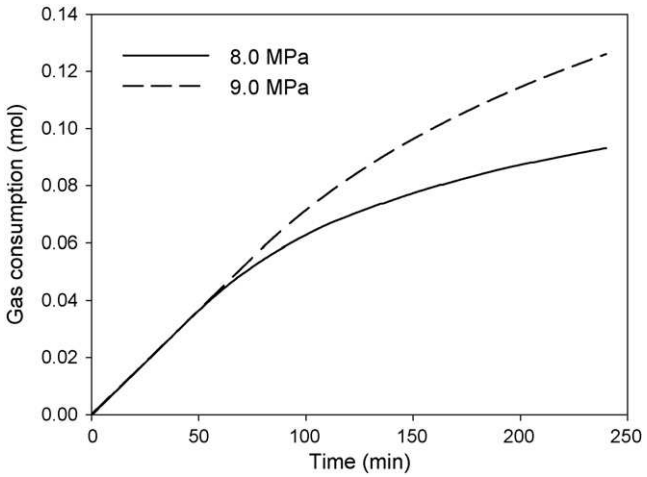

Fig. 3. Gas uptake measurement curves for hydrate formation in 100.0 nm silica gel pores (gel #2) at 272.15 K and 8.0 MPa (experiment 5) and 9.0 MPa (experiment 4).

also observed that gel #2 (100 nm) yields more hydrate at similar operating conditions compared to gel #1 (30 nm). The gas consumption is approximately three times higher for gel #2 at 9.0 MPa and five times higher at 8.0 MPa compared to gel #1. Table 3 shows the gas phase composition during hydrate formation for the 100 nm gel (gels #2 and #3). Experiments conducted with gel #2 show that CO_2 concentrations reduce from an initial value of 17% to 11.27% and 11.29% for the 8 and 9 MPa experiments respectively. Gas phase composition for gel #3 which has the same pore size as gel #2 but different particle sizes also shows similar CO_2 concentrations at the end of the experiment. Hence, the CO_2 concentration in the gas phase during a kinetic experiment was found to be 14.7%, 11.3% and 10.5% for gels #1, #2 and #3, respectively in 240 min of hydrate formation for the experiments conducted at 8 and 9 MPa (Table 3). Linga et al. (2007b) reported a CO_2 composition of 9.7% and 10.9% for experiments conducted at 10 and 11 MPa after 2 h of hydrate formation. They also observed that in a stirred vessel, the gas consumption reaches a plateau after 2 h of hydrate formation due to crystal agglomeration at the gas/liquid interface.

After the end of each kinetic experiment, the hydrate was decomposed, and the CO_2 content of the evolved gas was determined by GC. In the 30 nm experiments, results indicate that the hydrates formed at 8.0 MPa contain a slightly higher proportion of CO_2 than the 9.0 MPa case as shown in Table 4. Pure CO_2 forms hydrate at lower pressure compared to pure N_2. Thus, it is plausible to expect that more CO_2 will go into the hydrate phase at the lower pressure. A similar trend was reported by Linga et al. (2007a). The same trend is observed for the 100 nm gel experiments with CO_2 concentrations of 46.7% and 44.8% obtained at 8 and 9 MPa respectively.

3.1.2. Effect of pore size and particle size distribution on hydrate formation kinetics

Figs. 4 and 5 show the effect of pore size and particle size distribution on hydrate formation kinetics at similar operating condition conducted at two different pressures (8.0 and 9.0 MPa). The results show a marked increase in the gas uptake for the 100 nm gel (gels #2 and #3) compared to the 30 nm gel (gel #1). The CO_2 composition in hydrate is also much better for gels #2 and #3 compared to gel #1 as seen in Table 4. Gels #1 and #2 have the same particle size distribution (45–75 μm) and pore volume, but different pore diameters. For the pore volume to remain the same, the larger pore of 100.0 nm diameter results in a lower internal surface area. Results from Figs. 4 and 5 and Table 4 indicate that although the internal surface area in the 100.0 nm gel is lower than that in the 30.0 nm silica, the increased pore diameter is more favorable for hydrate formation. Gel #3 has 100.0 nm diameter pores, the same pore volume (0.83 ml/g) as gels #1 and #2 (0.81 ml/g) but a larger particle size distribution of 75–200 μm. The final CO_2 concentrations with gel #3 were 10.20% and 10.83% for the 8.0 and 9.0 MPa experiments respectively (Table 3). These values are less than the 11.27% and 11.29% obtained at the same experimental conditions for gel #2 (100.0 nm 40–75 μm). Fig. 6 shows the comparison of the performance of the three gels based on final gas consumption and the CO_2 composition of the residual gas composition at the end of the experiment. It is evident from the figure that the performance of the gel #3 is better than the other

Table 3
Gas phase CO_2 measurements during hydrate formation.

Time (min)	Gel #1			Gel #2		Gel #3	
	Experiment 3 (8.0 MPa)	Experiment 1 (9.0 MPa)	Experiment 2 (9.0 MPa)	Experiment 5 (8 MPa)	Experiment 4 (9 MPa)	Experiment 8 (8 MPa)	Experiment 6 (9 MPa)
	CO_2 (%) (±0.20)						
0	17.00	17.00	17.00	17.00	17.00	17.00	17.00
30	16.82	16.94	16.81	16.89	15.66	17.03	16.92
60	16.54	16.85	16.65	15.25	15.25	16.75	16.36
90	16.19	16.77	16.36	13.55	14.12	15.48	14.89
120	15.49	16.36	16.16	12.49	13.50	14.16	13.94
150	15.18	16.00	15.07	12.08	12.97	12.78	12.12
180	15.04	15.62	15.04	11.70	12.45	12.06	11.01
210	15.03	15.34	15.02	11.57	11.57	11.14	10.49
240	14.87	14.72	14.70	11.27	11.29	10.83	10.20

Please cite this article in press as: Adeyemo A, et al. Capture of carbon dioxide from flue or fuel gas mixtures by clathrate crystallization in a silica gel column. Int. J. Greenhouse Gas Control (2009), doi:10.1016/j.ijggc.2009.11.011

Table 4
Hydrate composition, CO_2 recovery and separation factor for gels #1, #2 and #3.

	Gel #1 30 nm (40–75 μm)		Gel #2 100 nm (40–75 μm)		Gel #3 100 nm (75–200 μm)	
	Exp. 3	Exp. 1	Exp. 5	Exp. 4	Exp. 8	Exp. 6
Pressure (MPa)	8.0	9.0	8.0	9.0	8.0	9.0
CO_2 in hydrate (mol%)	42.44	38.37	46.73	44.80	47.96	45.51
Split fraction or CO_2 recovery	0.16	0.21	0.42	0.41	0.45	0.51
Separation factor	8.42	3.20	5.82	3.69	9.86	8.22

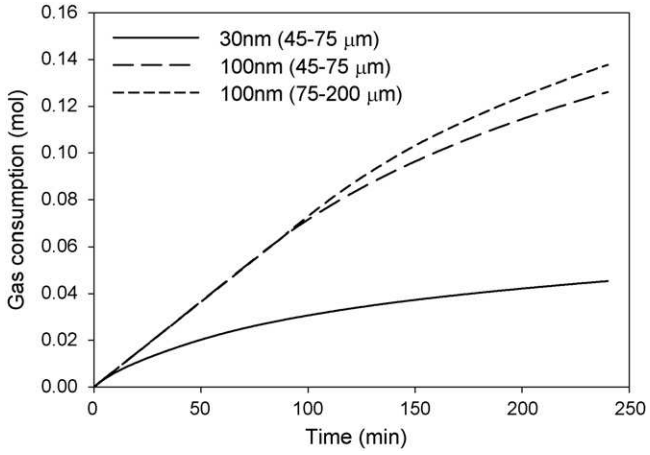

Fig. 4. Comparison of gas uptake measurement curves for hydrate formation at 9 MPa in gel #1 (experiment 1), gel #2 (experiment 4) and gel #3 (experiment 6) at 272.15 K.

gels. This is also confirmed by the higher CO_2 hydrate composition obtained for gel #3 given in Table 4. It is clear from the results that larger gel particles improve gas uptake and CO_2 separation.

Seo et al. (2005) postulated that CO_2 transported from the gas phase diffuses into the pores to participate in hydrate formation. Diffusion rates of gases through porous materials can be significantly lower than through air, and would depend on the properties of the medium such as porosity, pore sizes and pore connections (Mu et al., 2008). Simulation results on a 3-D bond pore network model by Mu et al. (2008) indicate that diffusivity increases with mean pore diameter when the pore size <1 μm as a result of the Knudsen effect, with a very strong dependence of effective diffusivity on pore size. Thus, it can be inferred that the increased hydrate formation observed in the 100 nm gel is because of increased diffusion in the larger pores. It has also been reported that hydrate equilibrium is also favorable at gels with larger pores compared to smaller ones (Kang et al., 2008).

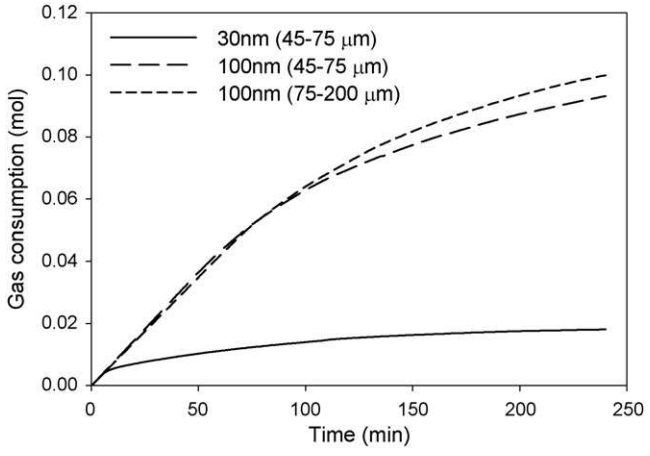

Fig. 5. Comparison of gas uptake measurement curves for hydrate formation at 8.0 MPa in gel #1 (experiment 3), gel #2 (experiment 5) and gel #3 (experiment 8) at 272.15 K.

3.1.3. Split fraction/CO_2 recovery

Linga et al. (2007a) presented two metrics to evaluate the separation process. Split fractions of 0.16 and 0.21 were obtained for the 30 nm experiment (Table 4). These low values indicate that 30 nm gel may not be a suitable medium for this process. Results from the 100 nm experiment show a split fraction of 0.42 and 0.41, respectively. It can also be seen in Table 4 that the 75–200 μm gel (#3) achieves the highest CO_2 capture at 8.0 MPa (45%) and at 9 MPa (51%). It is noted that Linga et al. (2007a) reported a CO_2 recovery of 42% for an experiment conducted in a stirred vessel at 273.7 K and 10.0 MPa. Even though the CO_2 recovery was more or less the same compared to a stirred vessel, the conversion of water to hydrate (44.5 for gel #3 at 9 MPa) was higher than the values (8.1–11.2%) obtained in the stirred vessel for 2 h (Linga, 2009). Hence, water present in silica gel pores presents a large area for gas/liquid contact thus resulting in higher gas consumption and subsequently higher yield (Seo et al., 2005). So far from the hydrate formation experiments conducted on three different gels at two different operating experimental pressures on the flue gas mixture,

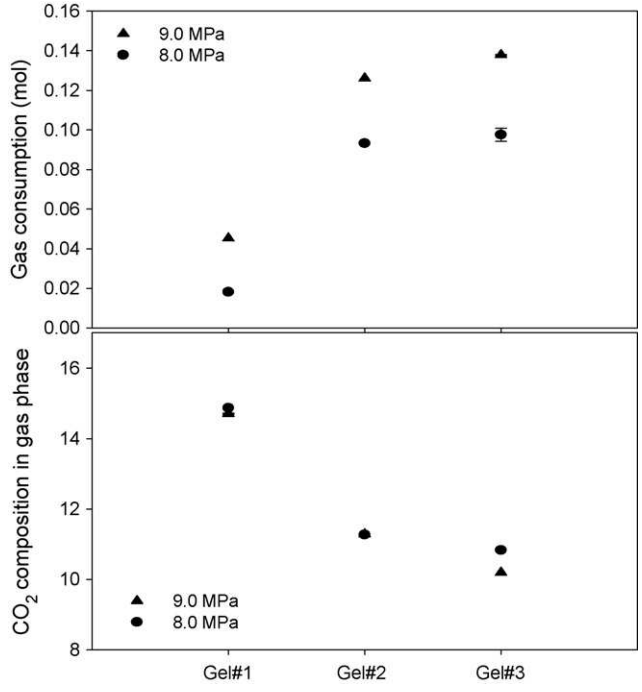

Fig. 6. Comparison of performance of the three gels based on final gas consumption (top) and the final residual gas phase composition of CO_2 (bottom). The end time for all the experiments is 240 min.

Please cite this article in press as: Adeyemo A, et al. Capture of carbon dioxide from flue or fuel gas mixtures by clathrate crystallization in a silica gel column. Int. J. Greenhouse Gas Control (2009), doi:10.1016/j.ijggc.2009.11.011

it was observed that gel #3 performed better in terms of gas consumption (Fig. 6), CO_2 capture in hydrate (Table 4), CO_2 recovery (Table 4), separation factor (Table 4) and conversion of water to hydrate (Table 2). The performance of gel #2 was much better than gel #1 but marginally lower than gel #3. Hence for the experiments conducted in the subsequent sections, only gel #3 was used.

3.1.4. Number of stages required to obtain high purity (>98%) CO_2 stream

In order to produce a high purity CO_2 stream suitable for sequestration or enhanced oil recovery additional hydrate stages are needed. The feed to the second stage would be the gas evolved from the hydrate formed in the first one. Hydrate formation experiments were carried out using a 45% CO_2–55% N_2 stream and silica gel #3 at −1 °C and 5.0 MPa. A lower operating pressure is now required since the increased per cent of CO_2 lowers the equilibrium formation pressure. A residual gas phase concentration of 28.2% CO_2 was obtained with a final hydrate phase composition of 71% CO_2. The CO_2 split fraction of 0.59 and the separation factor of 7.82 shows a better CO_2 recovery in the second stage compared to first one. In light of these results, a third stage of hydrate formation for a CO_2 (71%)/N_2 (29%) gas mixture was carried out at 2.7 MPa and −1 °C. The third stage of hydrate formation achieved a final hydrate concentration of 98.8% CO_2, with a split fraction of 0.56 and separation factor of 83.18. The high selectivity for CO_2 in third stage is due to the fact that the feed gas is rich in CO_2. Thus, after three hydrate formation/decomposition stages a 98.8% CO_2 stream can be produced.

3.1.5. CO_2/N_2 hydrate formation in the presence of THF

The high operating pressure remains a drawback of a hydrate process (Linga et al., 2007a). It is thus desirable to evaluate the CO_2 capture performance in the presence of THF in a silica gel column. One mol% THF aqueous solutions were used in this study. Previous work on a semi-batch stirred tank reactor indicated that 1.0 mol% is an optimal amount for the flue gas separation based on hydrate formation (Linga, 2009; Linga et al., 2008). The experiments were conducted using gel #3 at 5.0 MPa and two temperatures 272.15 and 274.15 K, respectively. This operating pressure which is 4.0 MPa lower than the maximum operating pressure without THF was selected after a number of trials to achieve an appreciable rate of hydrate formation (Adeyemo, 2008). The gas uptake measurements are shown in Fig. 7 along with a gas uptake curve obtained without THF at the same temperature but at 9 MPa. As seen in the figure, the gas consumption for the THF experiment tapers off at ~50 min with marginal incremental consumption observed beyond this point, compared to the experiment at 9.0 MPa (without THF) where the gas consumption curve is still on an upward trend after 240 min. The final gas uptake is significantly reduced in the system with THF (~10 times lower). The gas phase composition was analyzed at different times during the experiment and is given in Table 5. The CO_2 concentration reduced from 17.0% to 14.7%, while the evolved gas from the decomposed hydrate contained 28.6% CO_2. On the other hand, when a flue gas mixture was subjected to hydrate formation in a stirred vessel with 1.0 mol% THF as an additive, the CO_2 concentration in the gas phase reduced from 17.0% to ~9.8% for experiments conducted at 273.7 K and at operating pressures of 1.0, 1.4 and 2.5 MPa, respectively (Linga et al., 2008). The observed results clearly indicate that the addition of THF in the silica gel column significantly affects the kinetics of hydrate formation and the separation efficiency.

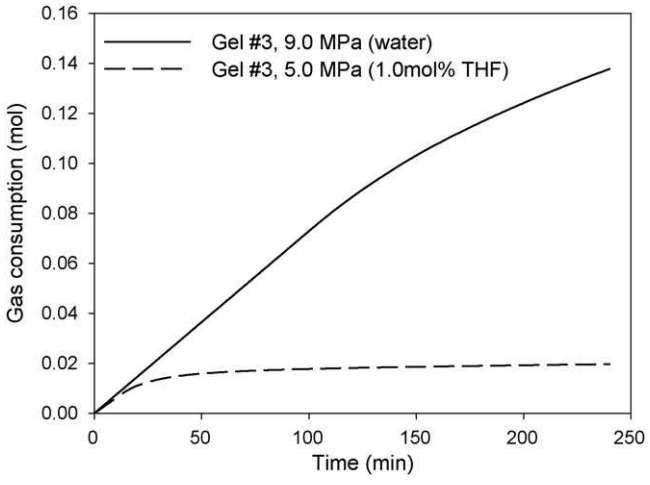

Fig. 7. Gas uptake curves for CO_2/N_2 (experiment 6) and CO_2/N_2/1.0 mol% THF (experiment 14) hydrate formation in 100.0 nm, 75–200 μm silica gel (gel #3).

Table 5
Gas phase CO_2 concentration during hydrate formation from the CO_2/N_2/THF (1.0 mol%) system with silica gel #3.

Gas phase CO_2 concentration for gel #3			
Experiment 14 (5.0 MPa)		Experiment 15 (5.0 MPa)	
Time (min)	CO_2 concentration (%) (uncertainty ± 0.20)	Time (min)	CO_2 concentration (%) (uncertainty ± 0.20)
0	17.00	0	17.00
30	16.79	30	16.96
60	16.76	60	16.76
90	16.66	90	16.58
120	16.29	120	15.85
150	15.84	150	15.65
180	15.34	180	15.36
210	14.91	210	14.87
240	14.78	240	14.72

3.2. Pre-combustion capture

The experimental conditions and results obtained for the fuel (CO_2/H_2) gas mixture with and without the presence of additive (THF) are given in Table 2. Fig. 8 shows the typical gas uptake curve obtained for the experiment conducted with gel #3 at 272.15 K and 7.0 MPa along with the temperature profile. As seen in the figure, the gas hydrate growth is constant up to 100 min and then gradually slows down. The conversion of water to hydrate of approximately 30% was achieved in 4 h of hydrate formation for the fuel gas mixture. On the other hand, hydrate growth in a semi-batch stirred tank reactor for this fuel gas mixture was found to be influenced by the agglomeration of hydrate particles at the gas/liquid interface and hence resulted in a conversion of water to hydrate of approximately 12% (Kumar, 2009; Linga et al., 2007b).

Gas consumption data from the experiments with CO_2/H_2 and CO_2/H_2/THF systems are shown in Fig. 9. Recently, kinetic experiments on a semi-batch stirred tank reactor for the fuel gas mixture in the presence of THF as an additive concluded that 1.0 mol% is the optimal amount (Lee et al., 2009) similar to the case of flue gas separation (Linga et al., 2008). Hence, 1.0 mol% THF aqueous solutions were used in the experiments with the silica gel. The final gas uptake is significantly reduced in the system with THF (~6 times lower). The gas uptake for the THF experiment tapers off at about 50 min where as for the experiment without additive, the gas consumption continues to increase due to hydrate formation. This resulted in a water conversion to hydrate of 30.4% for the experiment conducted without additive where as it was only 9.05% for the experiment conducted with THF. This significant decrease can be attributed to the presence of THF in some of the large cages

Please cite this article in press as: Adeyemo A, et al. Capture of carbon dioxide from flue or fuel gas mixtures by clathrate crystallization in a silica gel column. Int. J. Greenhouse Gas Control (2009), doi:10.1016/j.ijggc.2009.11.011

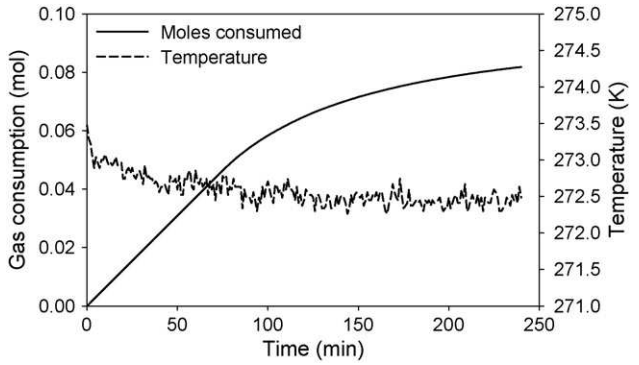

Fig. 8. Typical gas uptake measurement curve for CO_2/H_2 gas mixture conducted with gel #3 at 272.15 and 7.0 MPa (experiment 19).

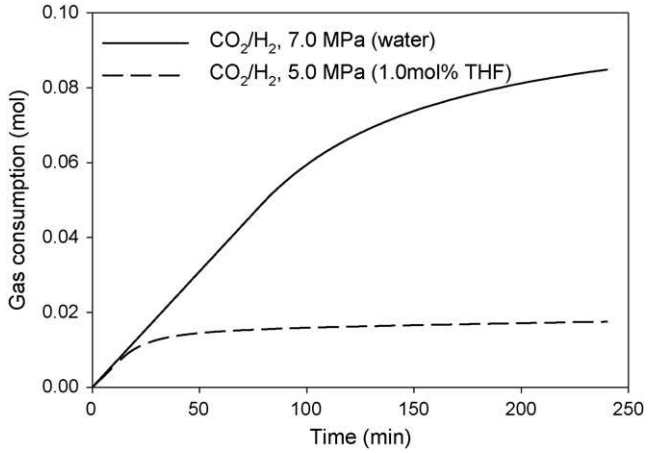

Fig. 9. Gas uptake curves for CO_2/H_2 (experiment 18) and CO_2/H_2/1.0 mol% THF (experiment 20) hydrate formation in 100.0 nm, 75–200 μm silica gel (gel #3).

of sII hydrate, thus reducing the available cavities for CO_2. A split fraction of 0.22 was obtained with THF compared with 0.61 without the additive. Thus, CO_2 is preferentially captured in the hydrate phase much more than H_2 especially in the absence of THF. Final residual gas phase concentration obtained after 4 h of hydrate formation with the presence of THF was 33.7% CO_2 and the decomposed hydrate contained 76.4% CO_2 (balance H_2). Recently, Lee et al. (2009) reported a similar hydrate composition for experiments conducted on a fuel gas mixture in the presence of 1.0 mol% THF employing a semi-batch stirred tank reactor. For the experiment conducted without THF the hydrate phase concentration was 92% whereas the residual gas phase concentration was 21.39% CO_2. These results show that hydrate formation using a silica gel column is more suited to separating fuel gas mixtures compared to that of flue gas mixtures. This is due in part to the higher initial CO_2 concentration compared to flue gas, and the lower affinity of hydrogen for the hydrate phase. Similar to the experiments conducted on the flue gas mixture, the presence of THF (1.0 mol%) significantly reduced the gas uptake and the separation efficiency. Finally, other applications such as gas separation of HFC-134a (Nagata et al., 2009) may also be considered.

4. Conclusions

Gas hydrate formation experiments from flue gas (CO_2/N_2) and fuel gas (CO_2/H_2) mixtures were carried out in a crystallizer using a column of silica gel particles. It was found that three stages of hydrate formation can achieve a 98.8 mol% CO_2 stream from a flue gas. Gels with larger pores and particle size were found to increase the gas consumption. The operating pressure can be reduced from 9.0 to 5.0 MPa with the addition of 1 mol% THF in the silica gel column. However, the rate of crystallization and separation efficiency as determined through the gas uptake and compositional analysis was significantly reduced. The experiments with the fuel gas showed that hydrate crystals containing 92 mol% CO_2 were formed. This indicates that the hydrate process may be more suited for the fuel gas mixtures compared to flue gases. Finally, it is concluded that the gel column performs as well as a stirred vessel in separating the gas components, however, the rate of gas uptake per mol of water and the hydrate yield are considerably enhanced in the former, and the need for costly stirring is eliminated.

Acknowledgement

The financial support from the Natural Sciences and Engineering Research Council of Canada (NSERC) is greatly appreciated.

References

Aaron, D., Tsouris, C., 2005. Separation of CO_2 from flue gas: a review. Sep. Sci. Technol. 40 (1–3), 321–348.
Adeyemo, A., 2008. Post Combustion Capture of Carbon Dioxide through Hydrate Formation in Silica Gel Column. University of British Columbia, Vancouver.
Bishnoi, P.R., Natarajan, V., 1996. Formation and decomposition of gas hydrates. Fluid Phase Equilib. 117 (1–2), 168–177.
Booras, G.S., Smelser, S.C., 1991. An engineering and economic-evaluation of CO_2 removal from fossil-fuel-fired power-plants. Energy 16 (11–12), 1295–1305.
Davidson, D.W., Leaist, D.G., Hesse, R., 1983. Oxygen-18 enrichment in the water of a clathrate hydrate. Geochim. Cosmochim. Acta 47, 2293.
Englezos, P., 1996. Nucleation and growth of gas hydrate crystals in relation to "Kinetic Inhibition". Rev. IFP 51 (6), 789.
Gudmundsson, J.S., Parlaktuna, M., Levik, O.I., Andersson, V., 2000. Laboratory for continuous production of natural gas hydrates. Gas Hydrates: Challenges for the Future 912, 851–858.
Hendriks, C.A., Blok, K., Turkenburg, W.C., 1991. Technology and cost of recovering and storing carbon-dioxide from an integrated-gasifier, combined-cycle plant. Energy 16 (11–12), 1277–1293.
Herzog, H.J., Drake, E.M., 1996. Carbon dioxide recovery and disposal from large energy systems. Annu. Rev. Energy Environ. 21, 145–166.
IPCC, 2005. Special report on carbon dioxide capture and storage, Intergovernmental Panel on Climate Change.
Kang, S.P., Lee, H., 2000. Recovery of CO_2 from flue gas using gas hydrate: thermodynamic verification through phase equilibrium measurements. Environ. Sci. Technol. 34 (20), 4397–4400.
Kang, S.P., Lee, H., Ryu, B.J., 2001. Enthalpies of dissociation of clathrate hydrates of carbon dioxide, nitrogen, (carbon dioxide plus nitrogen), and (carbon dioxide plus nitrogen plus tetrahydrofuran). J. Chem. Thermodyn. 33 (5), 513–521.
Kang, S.P., Lee, J.W., Ryu, H.J., 2008. Phase behavior of methane and carbon dioxide hydrates in meso- and macro-sized porous media. Fluid Phase Equilib. 274 (1–2), 68–72.
Klara, S.M., Srivastava, R.D., 2002. US DOE integrated collaborative technology development program for CO_2 separation and capture. Environ. Prog. 21 (4), 247–253.
Kumar, R., 2009. Separation of carbon dioxide from fuel gas mixture (pre combustion capture) via hydrate crystallization. Manuscript Thesis, University of British Columbia, Vancouver.
Kumar, R., Englezos, P., Moudrakovski, I., Ripmeester, J.A., 2009. Structure and composition of CO_2/H_2 and $CO_2/H_2/C_3H_8$ hydrate in relation to simultaneous CO_2 capture and H_2 production. AIChE J. 55 (6), 1584–1594.
Kumar, R., Linga, P., Moudrakovski, I., Ripmeester, J.A., Englezos, P., 2008. Structure and kinetics of gas hydrates from methane/ethane/propane mixtures relevant to the design of natural gas hydrate storage and transport facilities. AIChE J. 54 (8), 2132–2144.
Lee, H.J., Lee, J.D., Linga, P., Englezos, P., Kim, Y.S., Lee, M.S., Kim, Y.D., 2009. Gas hydrate formation process for pre-combustion capture of carbon dioxide. Energy, doi:10.1016/j.energy.2009.05.026.
Lee, J.D., Susilo, R., Englezos, P., 2005. Kinetics of structure H gas hydrate. Energy Fuels 19 (3), 1008–1015.
Lee, S., Liang, L.Y., Riestenberg, D., West, O.R., Tsouris, C., Adams, E., 2003. CO_2 hydrate composite for ocean carbon sequestration. Environ. Sci. Technol. 37 (16), 3701–3708.
Linga, P., 2009. Separation of carbon dioxide from flue gas (post combustion capture) via hydrate crystallization. Manuscript Thesis, University of British Columbia, Vancouver.
Linga, P., Adeyemo, A., Englezos, P., 2008. Medium-pressure clathrate hydrate/membrane hybrid process for postcombustion capture of carbon dioxide. Environ. Sci. Technol. 42 (1), 315–320.

Please cite this article in press as: Adeyemo A, et al. Capture of carbon dioxide from flue or fuel gas mixtures by clathrate crystallization in a silica gel column. Int. J. Greenhouse Gas Control (2009), doi:10.1016/j.ijggc.2009.11.011

Linga, P., Kumar, R., Englezos, P., 2007a. The clathrate hydrate process for post and pre-combustion capture of carbon dioxide. J. Hazard. Mater. 149 (3), 625–629.
Linga, P., Kumar, R., Englezos, P., 2007b. Gas hydrate formation from hydrogen/carbon dioxide and nitrogen/carbon dioxide gas mixtures. Chem. Eng. Sci. 62 (16), 4268–4276.
McCallum, S.D., Riestenberg, D.E., Zatsepina, O.Y., Phelps, T.J., 2007. Effect of pressure vessel size on the formation of gas hydrates. J. Petrol. Sci. Eng. 56 (1–3), 54–64.
Mori, Y.H., 2003. Recent advances in hydrate-based technologies for natural gas storage—a review. J. Chem. Ind. Eng. (China) 54, 1–17.
Mu, D., Liu, Z.-S., Huang, C., Djilali, N., 2008. Determination of the effective diffusion coefficient in porous media including Knudsen effects. Microfluid. Nanofluid. 4 (3), 257–260.
Nagata, T., Tajima, H., Yamasaki, A., Kiyono, F., Abe, Y., 2009. An analysis of gas separation processes of HFC-134a from gaseous mixtures with nitrogen—comparison of two types of gas separation methods, liquefaction and hydrate-based methods, in terms of the equilibrium recovery ratio. Sep. Purif. Technol. 64 (3), 351–356.
Ohmura, R., Kashiwazaki, S., Shiota, S., Tsuji, H., Mori, Y.H., 2002. Structure-I and structure-H hydrate formation using water spraying. Energy Fuels 16 (5), 1141–1147.
Park, J., Seo, Y.T., Lee, J.W., Lee, H., 2006. Spectroscopic analysis of carbon dioxide and nitrogen mixed gas hydrates in silica gel for CO_2 separation. Catal. Today 115 (1–4), 279–282.
Ripmeester, J.A., Ratcliffe, C.I., 1988. Low-temperature cross-polarization/magic angle spinning carbon-13 NMR of solid methane hydrates: structure, cage occupancy, and hydration number. J. Phys. Chem. 92 (2), 337–339.
Seo, Y.T., Moudrakovski, I.L., Ripmeester, J.A., Lee, J.W., Lee, H., 2005. Efficient recovery of CO_2 from flue gas by clathrate hydrate formation in porous silica gels. Environ. Sci. Technol. 39 (7), 2315–2319.
Sloan Jr., E.D., 1998. Clathrate hydrates of natural gases. In: Revised and Expanded, second ed. Marcel Dekker, NY, 754 pp.
Sum, A.K., Burruss, R.C., Sloan, E.D., 1997. Measurement of clathrate hydrates via Raman spectroscopy. J. Phys. Chem. B 101 (38), 7371–7377.
Susilo, R., Ripmeester, J.A., Englezos, P., 2007a. Characterization of gas hydrates with PXRD, DSC, NMR, and Raman spectroscopy. Chem. Eng. Sci. 62 (15), 3930–3939.
Susilo, R., Ripmeester, J.A., Englezos, P., 2007b. Methane conversion rate into structure H hydrate crystals from ice. AlChE J. 53 (9), 2451–2460.
Tsouris, C., Brewer, P., Peltzer, E., Walz, P., Riestenberg, D., Liang, L.Y., West, O.R., 2004. Hydrate composite particles for ocean carbon sequestration: field verification. Environ. Sci. Technol. 38 (8), 2470–2475.
Tsouris, C., Szymcek, P., Taboada-Serrano, P., McCallum, S.D., Brewer, P., Peltzer, E., Walz, P., Adams, E., Chow, A., Johnson, W.K., Summers, J., 2007. Scaled-up ocean injection of CO_2-hydrate composite particles. Energy Fuels 21 (6), 3300–3309.
Tsuji, H., Ohmura, R., Mori, Y.H., 2004. Forming structure-H hydrates using water spraying in methane gas: effects of chemical species of large-molecule guest substances. Energy Fuels 18 (2), 418–424.
Uchida, T., Ebinuma, T., Narita, H., 2000. Observations of CO_2-hydrate decomposition and reformation processes. J. Cryst. Growth 217 (1/2), 189–200.
Uchida, T., Hirano, T., Ebinuma, T., Narita, H., Gohara, K., Mae, S., 1999. Raman spectroscopic determination of hydration number of methane hydrates. AlChE J. 45 (12), 2641–2645.
Udachin, K.A., Lu, H., Enright, G.D., Ratcliffe, C.I., Ripmeester, J.A., Chapman, N.R., Riedel, M., Spence, G., 2007. Single crystals of naturally occurring gas hydrates: the structures of methane and mixed hydrocarbon hydrates. Angew. Chem. Int. Ed. 46 (43), 8220–8222.
Udachin, K.A., Ratcliffe, C.I., Ripmeester, J.A., 2001. Structure, composition, and thermal expansion of CO_2 hydrate from single crystal X-ray diffraction measurements. J. Phys. Chem. B 105 (19), 4200–4204.
Wang, X.P., Schultz, A.J., Halpern, Y., 2002. Kinetics of methane hydrate formation from polycrystalline deuterated ice. J. Phys. Chem. A 106 (32), 7304–7309.
West, O.R., Tsouris, C., Liang, L., 2001. Method and apparatus for efficient injection of CO_2 in oceans, United States Patent# 6,598,407.

Please cite this article in press as: Adeyemo A, et al. Capture of carbon dioxide from flue or fuel gas mixtures by clathrate crystallization in a silica gel column. Int. J. Greenhouse Gas Control (2009), doi:10.1016/j.ijggc.2009.11.011